Transient competition between photocatalysis and carrier recombination in TiO_2 nanotube film loaded with Au nanoparticles*

Shao Zhu-Feng(邵珠峰)[a)b)], Yang Yan-Qiang(杨延强)[a)], Liu Shu-Tian(刘树田)[a)†], and Wang Qiang(王 强)[a)b)‡]

[a)] *Department of Physics, Harbin Institute of Technology, Harbin* 150001, *China*

[b)] *Department of Optics and Electronics Science, College of Science, Harbin Institute of Technology at Wei Hai, Weihai* 264209, *China*

(Received 20 December 2013; revised manuscript received 3 March 2014; published online 16 July 2014)

Highly ordered TiO_2 nanotube array (TNA) films are fabricated by using an anodic oxidation method. Au nanoparticles (NPs) films are decorated onto the top of TNA films with the aid of ion-sputtering and thermal annealing. An enhanced photocatalytic activity under ultraviolet C (UVC, 266 nm) light irradiation is obtained compared with that of the pristine TNA, which is shown by the steady-state photoluminescence (PL) spectra. Furthermore, a distinct blue shift in the nanosecond time-resolved transient photoluminescence (NTRT-PL) spectra is observed. Such a phenomenon could be well explained by considering the competition between the surface photocatalytic process and the recombination of the photo-generated carriers. The enhanced UV photocatalytic activities of the Au–TNA composite are evaluated through photo-degradation of methyl orange (MO) in an aqueous solution with ultraviolet–visible absorption spectrometry. Our current work may provide a simple strategy to synthesize defect-related composite photocatalytic devices.

Keywords: TiO_2 nanotube array film, Au nanoparticles, oxygen vacancies, photocatalytic activity

PACS: 61.72.Ji, 68.37.HK, 81.07.De, 81.16.Hc **DOI:** 10.1088/1674-1056/23/9/096102

1. Introduction

Owing to its non-toxicity, low cost, availability, and high stability, titanium dioxide (TiO_2) has recently been explored for a wide range of functional applications, ranging from photocatalysis,[1] solar energy conversion,[2] electrochromic effects,[3] second-order nonlinear optical elements,[4] to use as a biomaterial.[5] In 1972, Fujishima and Honda first reported that water can be decomposed directly by irradiating the TiO_2 surface with the incident ultraviolet light of a wavelength shorter than 190 nm,[6] which opens up the promising potential of TiO_2 for photocatalytic applications, such as the elimination of environmental pollutants from water and air and the photo-induced killing of micro-organisms.[7] Nowadays, a new trend in the science of TiO_2 for initiating the visible-light driven photocatalytic processes has aroused great research interest, in consideration of both the energy crisis and the danger of ultraviolet (UV) light. As we know, there are three main crystalline structures (anatase, rutile, and brookite) for TiO_2, especially, the band gaps of the anatase and the rutile structures are 3.2 eV and 3.0 eV, respectively. Thus, it requires ultraviolet illumination to initiate the photocatalytic and the photo-electricity conversion processes, and the energy gaps are both rather large for efficiently harvesting the visible solar light.[8] Moreover, the practical photocatalytic and photo-electricity conversion applications of TiO_2 are limited by its low quantum efficiency as a result of the fast recombination of photo-generated carriers. Therefore, a new kind of photocatalytic TiO_2-based material must be designed to cater to the requirements of a high visible-light-harvesting ability and efficient interfacial carrier separation.

The photocatalytic properties of TiO_2 can be improved by introducing defect states, especially oxygen vacancies (OVs),[9] which can extend the light absorption of TiO_2 from UV to the visible or even infrared regions.[10] However, some researchers believe that OVs in TiO_2 act as a recombination center for the photo-generated electron–hole (e^-–h^+) pairs, which will lower the photocatalytic activity.[11] It is due to the low electron mobility in these sites and the fact that the energy level of OV is located in the intraband. One of the promising strategies to overcome the above drawback is the incorporation of noble metal nanoparticles (NPs), such as Pt, Pd, Au, and Ag, to facilitate the e^-–h^+ separation and promote the interfacial electron transfer process that in turn increases the surface reactivity.[12–15] This metal–semiconductor (M–S) composite can result in an efficient separation of the photo-generated charge carriers by forming a Schottky barrier at the nano junctions between the semiconductor and the metal NPs, which suppresses the charge recombination process to improve the photocatalytic activity. TiO_2 nano tube array (TNA) films grown by the anodization of titanium have attracted much attention in the above consideration due to the unique microstructure of bundled nano tubes standing on a metallic Ti substrate, which shows a high surface to volume

*Project supported by the National Natural Science Foundation of China (Grant No. 11274082) and the Shandong Excellent Young Scientist Research Award Fund Project, China (Grant No. BS2011CL002).

†Corresponding author. E-mail: stliu@hit.edu.cn

‡Corresponding author. E-mail: wq19750505@tom.com

© 2014 Chinese Physical Society and IOP Publishing Ltd

ratio and a precisely controllable morphology. As can be easily foreseen, it is more convenient for the separation of photo-induced charge when compared to the TiO_2 NPs, and the composite of a TNA film with noble metal NPs can be prefigured as an ideal candidate to promote the photocatalytic activities. To the best of our knowledge, the research in this trend is seldom carried out. Moreover, the ultrafast dynamics process for the interfacial charge separation remains unknown, which is physically adverse for designing the optimal microstructure of a TNA–noble metal NPs composite.

Here, a TNA film decorated with an Au NPs film is obtained, which is shown by the steady-state PL spectrum to have an enhanced photocatalytic activity under ultraviolet C (UVC, 266 nm) light irradiation compared with the pristine sample. This observation suggests that Au NPs really work for suppressing the photo-generated e^-–h^+ pair recombination and improvement of the photocatalytic activity. Furthermore, a distinct blue-shift phenomenon in the nanosecond time-resolved transient photoluminescence (NTRT-PL) spectra is observed. To the best of our knowledge, there are few reports for this interesting phenomenon, which is well explained by introducing competition mechanisms between the photocatalytic process and the photo-generated carrier recombination at the interfaces of the TNA–Au composite.

2. Experiments

TiO_2 nanotube array films, formed by the tight bonding of hexagonally-structured nanotubes, were synthesized by the anodization of Ti foils in an electrolyte containing water, NH_4F (0.45 wt.%), and ethanediol (98 vol.%), which was described previously.[16] Coating of an ultra-thin Au film on the air-dried TNA film was performed using an ion-sputtering system, and the isolated Au NPs on the TNA film were formed by thermal annealing in a tubular furnace with different spurting time (10 s, 20 s, 40 s, and 60 s respectively). The highest ramp speed of the temperature in the furnace was 10 °C/min. When the preset temperature (400 °C) was reached, the samples were pushed into the flat-temperature zone manually, and they were annealed for 0.5 h. Well-controlled sample preparations are critical to form nice structures of well-separated Au nanoparticles on the TiO_2 nanotube. The microstructures of the TNA decorated with Au NPs were investigated using scanning electron microscopy (SEM: Hitachi S4200) with an accelerating voltage of 15.0 kV.

The crystal structure of the TiO_2 nanotube was investigated by using a JY-T64000 micro-Raman spectroscopy system with Ar^+ laser excitation (514.5 nm), and the oxidation states of Ti at the TNA film surface were examined by X-ray photoelectron spectroscopy (XPS, ESCALAB 250) using a Thermo Fisher Scientific Ltd. (TFS) instrument. The X-ray source was an Al anode emitting the $K\alpha$ (1486.6 eV) radiation at 150 W.

A Ti:sapphire femtosecond laser system (Spectra-Physics) was used to excite the steady-state and the NTRT-PL spectra. The excitation beam centered at 266 nm was acquired by frequency doubling of the 532 nm laser beam through a BBO (beta-BaB_2O_4, barium metaborate) crystal, with a pulse duration of 130 fs, a repetition rate of 1 kHz, and a spot size of 1 mm. The emission was collected by a spectrometer (Bruker Optics 250 IS/SM) coupled with an intensified charge-coupled device (CCD) detector (IStar740, Andor). The steady-state and the nanosecond time-resolved experiments were carried out by adjusting the delay time of the CCD shutter. The laser pulse gave an external trigger signal to open 100 ms and 0.5 ns temporal gate of the intensified CCD through a synchronization/delay generator (SDG) and a digital delay/pulse generator (DG535), then the steady-state and the transient PL spectra at the different decay time could be recorded by the CCD detector, respectively. However, there were two large-intensity noise peaks at 400 nm and 532 nm, which concealed the desired signals. The noise peaks at 400 nm and 532 nm originated from the frequency doubling and the first-order diffraction of the CCD detector grating, respectively. Therefore, these two peaks were deleted from the as-measured NTRT-PL spectra. Figure 1 gives a schematic diagram of the experimental setup.

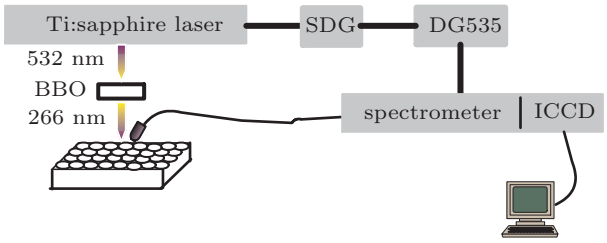


Fig. 1. (color online) Experiment setup of nanosecond time resolved PL measurement.

The photocatalytic activities of pristine TNA and Au NPs decorated TNA films were investigated using the photo degradation of methyl orange (MO) under UV irradiation (wavelength: 254 nm, electrical power: 11 W). MO (5 mg) was dissolved in 500 mL de-ionized water to yield a solution with a methyl orange concentration of 10 mg/L. The concentration of the MO solution was measured every 2 hours by monitoring the intensity variation of the characteristic absorption peak at 464 nm using a UV–vis spectrophotometer.

3. Results and discussion

Figure 2(a) shows the top-view SEM image of the TiO_2 NTs film, which shows the open top of the NTs with a thin sidewall thickness of about 20 nm and a pore diameter of less than 100 nm. Figure 2(b) shows the bottom-view SEM image of the NTs, where most NTs show hexagonal patterns and some others show irregular pentagonal patterns. Figures 2(c)–2(f) show the morphologies of the TiO_2 NTs film after Au coating and annealing at 400 °C with different sputtering time (10 s, 20 s, 40 s and 60 s, respectively), exhibiting a well-isolated gold NPs film, which is formed by thermal migration and re-condensation of the original continuous gold granular.[17]

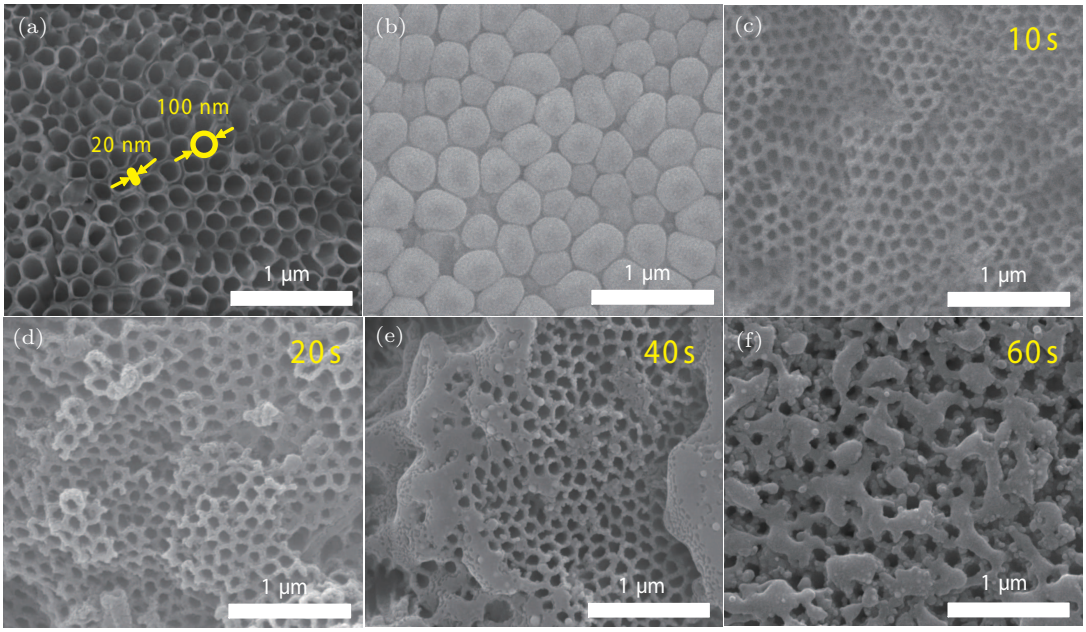


Fig. 2. (color online) SEM images of TiO_2 NTs film: (a) top-view picture, (b) bottom-view picture. (c)–(f) Au NPs film on TNA after annealing at 400 °C with different sputtering times of 10 s, 20 s, 40 s, and 60 s, respectively.

The strong interaction between gold NPs and TiO_2 is beneficial for the effective separation of the photo-generated electron–hole pairs, which is ascertained by the following PL spectrum analysis and in turn could lead to an enhanced photocatalytic performance. The PL emission spectrum is useful to disclose the efficiencies of charge carrier trapping, migration, and transfer, since the PL emission mainly results from the recombination of the photo-excited free carriers.[18] Figure 3 shows the steady-state PL spectra of the Au NPs-decorated TNA films with different sputtering times (0 s, 10 s, 20 s, 40 s, and 60 s). In the tested spectral region, the emission peak at 470 nm results from the existence of surface states in TiO_2.[18] It can be seen that the peak positions in the PL spectrum of the Au NPs-decorated TNA film are in agreement with those of the pristine TNA film. However, the PL intensities are quite sensitive to the Au NPs modification, just as shown in Fig. 3. In general, a lower PL intensity indicates a lower radiative recombination rate of the electron–hole pairs under the same irradiation. The PL intensities of the Au NPs decorated TNA films are much lower than those of the pristine TNA sample, demonstrating that the Au NPs effectively suppress the radiative charge recombination in the composted films.

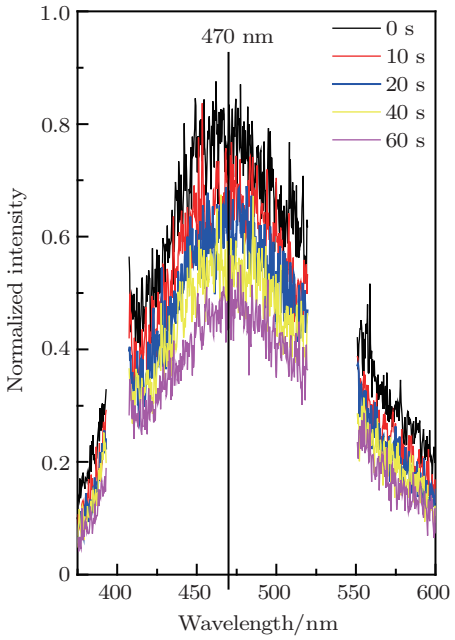


Fig. 3. (color online) Steady-state PL spectra of the prepared TNA film samples with different sputtering times.

We use NHE to denote the normal hydrogen electrode. Since the conduction band energy of TiO_2 (−0.29 V vs.

NHE) is higher than the Fermi level of Au (+0.5 V vs. NHE), electrons are driven from the conduction band of TiO_2 to the Au NPs by an interfacial electric field in the Schottky nano junctions. Then, the oxygen molecules adsorbed on the Au NPs surface are reduced to superoxide anions ($\cdot O^{2-}$) by the photo-generated electrons in a normal oxygen-bearing circumstance.[19] Therefore, the direct recombination of photo-generated electron–hole can be prevented. It is well known that the PL emission results from the radiative recombination of the photo-generated electron–hole. Consequently, it is reasonable that the PL intensities of the Au NPs decorated TNA film are much lower than those of the TNA film. This result suggests that the Au NPs on the TNA surface are able to extract electrons from the conduction band of TiO_2 to reduce the oxygen molecule adsorbed on the Au NPs, which resultantly prevent the charge carrier recombination.

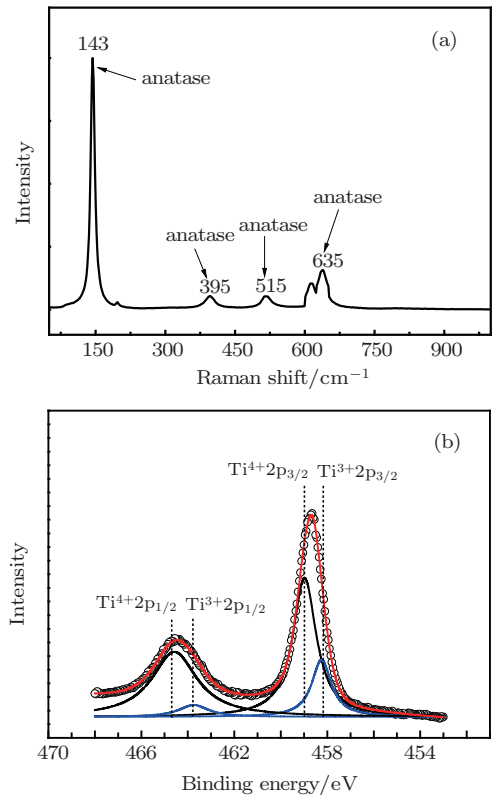


Fig. 4. (color online) (a) Raman spectra of TNA film without Au NPs, the reference Raman peaks are also shown. (b) Theoretical fit of Ti 2p XPS spectrum for TNA film without Au NPs.

Raman spectra and X-ray photoelectron spectroscopy (XPS) for the TNA film without Au NPs are presented in Fig. 4. Figure 4(a) shows a distinct Raman band over the spectral range of 100–900 cm^{-1}. The Raman spectrum of the sample consists of peaks at 143 cm^{-1}, 395 cm^{-1}, 515 cm^{-1}, and 635 cm^{-1}, which can be attributed to the anatase structure. From the analysis of the Raman peak positions, it can be concluded that the anatase polymorphic form predominates in the film.[20] The Raman spectroscopy measurements remain in good agreement with the X-ray diffraction (XRD) analysis, which has been published previously.[16] Figure 4(b) shows the results of the XPS measurement. The black-hollow circles are the experimental data points, and the red-solid line is the result of curve fitting. The Ti 2p spectra are decomposed into two components originating from Ti^{4+} and Ti^{3+}, including Ti^{4+} $2p_{1/2}$, Ti^{3+} $2p_{1/2}$, Ti^{4+} $2p_{3/2}$, and Ti^{3+} $2p_{3/2}$.[21] The Ti^{4+} state is connected with the stoichiometric TiO_2. On the other hand, Ti^{3+} is an intermediate oxidation state (Ti_2O_3). It obviously indicates the presence of OV in the as-formed TNA film.

Generally, the photocatalytic reaction can be considered to be the continuous processes of generation, transfer, and consumption of photo-generated charge carriers. Any approach that could enhance each step in the process would improve the ultimate photochemical reaction. Of course, there are many methods to characterize the photocatalytic performance improvement of a designed structure, such as, the color changing of a reduction object,[22] the percentage photo degradation of a reduction object,[23] and the amount of evolved hydrogen.[24] As we see, the above methods are indirect for characterizing the charge transfer, and a more direct method of transient photoluminescence spectrum is proposed extensively to study the nature of charge transfer in metal–semiconductor nano junctions.

We have adopted the method of transient photoluminescence spectrum to evaluate the charge transfer in the Au NPs-decorated TNA films. Figures 5(a)–5(e) show a distinct blue shift of the emission peak in the NTRT-PL spectra with different Au sputtering times. In each picture, the NTRT-PL spectrum time interval is 1.5 ns. As shown previously, the enhanced photocatalytic activity of the Au NPs decorated TNA results from the efficient separation and transfer of the photo-generated charge carriers. In the case of the pristine TNA in the dark, molecular oxygen in the atmosphere is adsorbed on the surface of TNA, and there is no charge transfer.[25] As a result, the surface energy band of TNA is rather flat, as shown in Fig. 6(a). In the case of the pristine TNA under UVC light irradiation, lots of electrons are promoted from the valence band across the band gap to the conduction band upon excitation since the wavelength of the incident photons, 266 nm ($E_g \approx 4.7$ eV), is much less than the threshold wavelength of TiO_2, 388 nm ($E_g \approx 3.2$ eV). When the UVC irradiation is carried out to aerated TiO_2 , partial photo-generated electrons are captured by the adsorbed oxygen molecules.[22] Certainly, there are still a large number of surplus electrons in the conduction band and vacancies in the valence band of TNA in the steady state. The surface energy band bending of TNA results from the charge transfer. It is illustrated in Fig. 6(b). In the case of the pristine TNA just after the UVC light irradiation, the evolution of the transient states appears in the NTRT-PL spectrum, which is the physical demonstration of the dynamic recombination process of the photo-generated e^-–h^+ pairs.

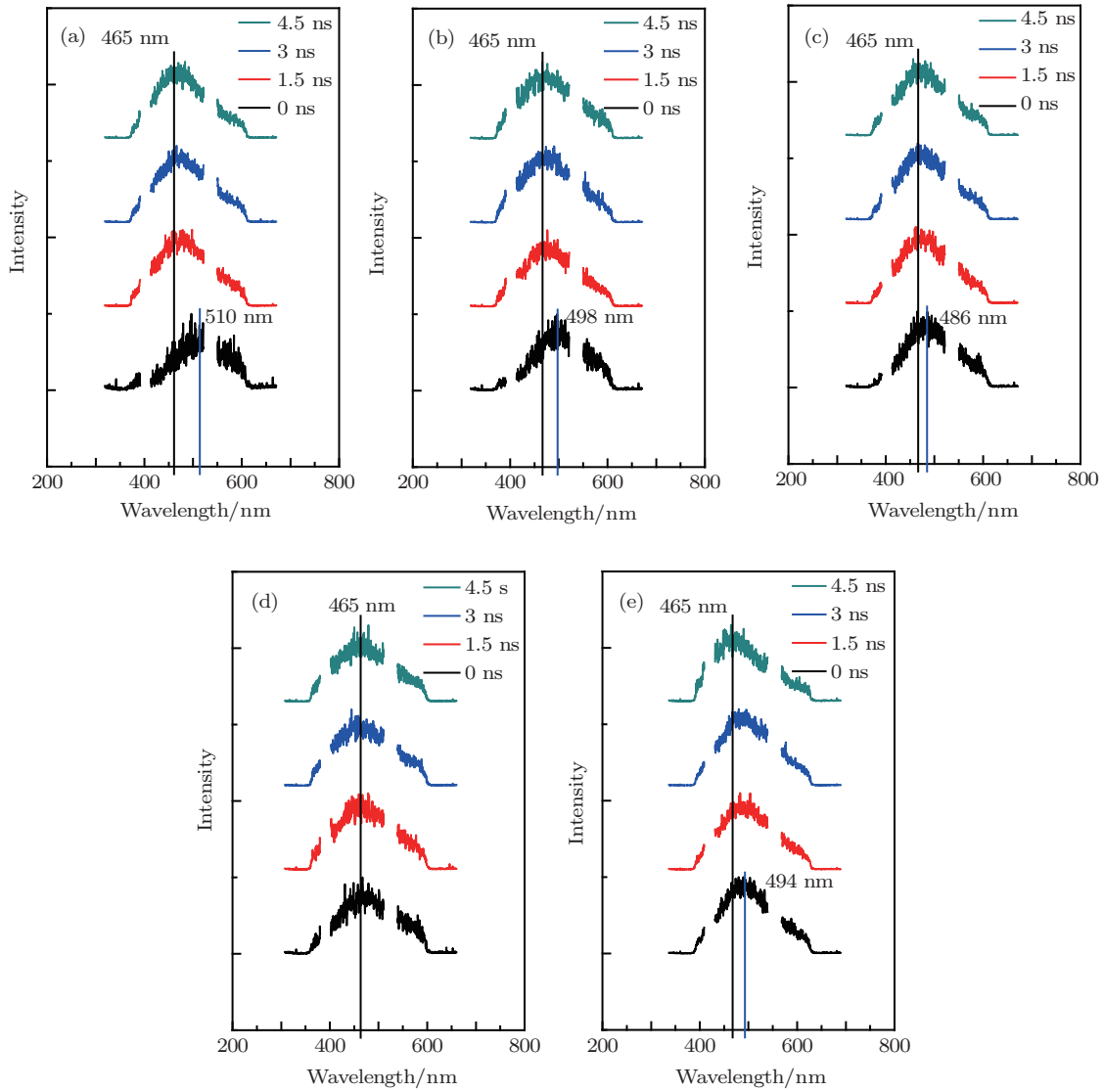


Fig. 5. (color online) Blue shifts in nanosecond time-resolved transient photoluminescence spectra with different sputtering times: (a) 0 s, (b) 10 s, (c) 20 s, (d) 40 s, (e) 60 s.

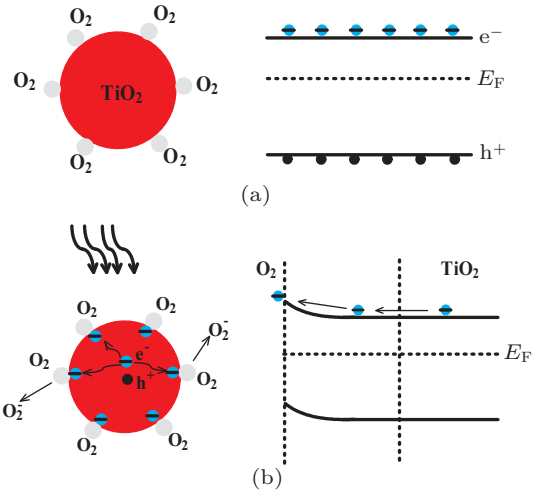


Fig. 6. (color online) (a) Schematic illustration of molecular oxygen adsorbed on the surface of pristine TNA under no irradiation and surface energy band of pristine TNA. (b) Schematic illustration of electrons transfer in pristine TNA under UVC light irradiation and surface energy band of pristine TNA under light irradiation.

Owing to the experimental fact that the steady-state PL peak is located at 470 nm, we can envisage the following procedure for the transient dynamics of photo charges in the Au–TNA nano composites, in consideration of the OV formation in the annealing process of TNA. It has been shown that the concentration of OV increases exponentially with increasing temperature.[26] In fact, it generates not a single oxygen vacancy energy level but a series of discrete vacancy oxygen energy levels in the band gap of TNA during the annealing process.[27] According to the previous study,[28,29] there are two kinds of oxygen vacancies that can contribute to the PL characteristic in TiO_2, i.e., the F center and the F^+ center. The F center represents the neutral oxygen vacancy, whereas the F^+ center represents the oxygen vacancy losing one electron. The transitions from the F center and the F^+ center to the valence band are located at 465 nm (2.7 eV) and 525 nm (2.4 eV) in the PL spectrum, respectively.[28] However, some others

have proposed that the transition from the oxygen vacancy energy level to the valence band produces an emission at 505 nm (2.45 eV).[29] This inconformity reveals that the oxygen vacancy produces a series of discrete energy levels rather than a single one.[30] Therefore, we have a sound reason to believe that the radiative transition from one of the OV levels to the valence band should produce the PL emission at 510 nm. The schematic distribution of both F and F^+ levels are shown in Fig. 7(a). Experimental and theoretical studies have revealed that an ionized oxygen vacancy level (F^+) can trap a photo-generated electron to rise back to the higher oxygen vacancy level (F).[30–32]

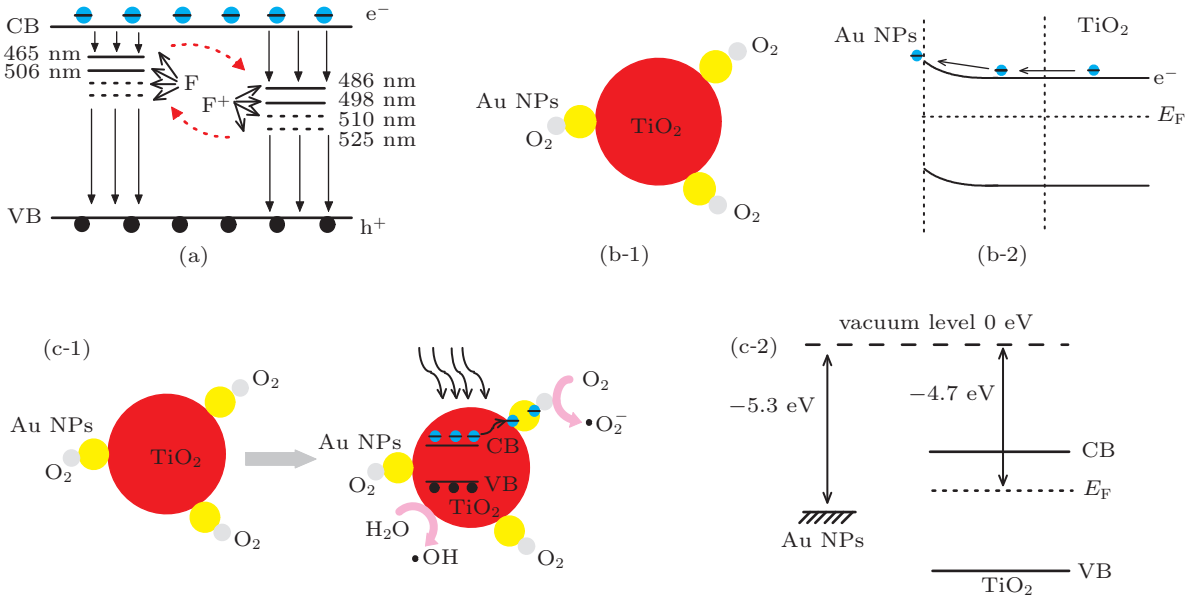


Fig. 7. (color online) (a) Schematic illustration of photo-generated electron–hole pair recombination process (transient process) after UVC light irradiation. (b-1) Molecular oxygen adsorption on Au NPs decorated TNA. (b-2) Schematic illustration of Schottky junction between metal and semiconductor and surface energy band of Au NPs decorated TNA. (c-1) Schematic illustration of photocatalytic process of Au NPs decorated TNA under UVC light irradiation, and (c-2) surface energy band of Au NPs decorated TNA under light irradiation.

Based on the above analysis and the experimentally observed blue-shifted transient PL emission, we now propose an applicable mechanism for the charge transfer in the TNA–Au composite. The photo-generated conduction band electrons (e^-_{CB}) with a rather high concentration almost fully accommodate both the F center levels and the lower F^+ center levels due to their low densities of states (DOS). The electrons subsequently combine with holes in the valence band (h^+_{VB}) and produce radiation at 510 nm. With the transiently decreased electron concentration, a larger percentage of electrons transit to the F center levels to radiate light at the shorter wavelength of 465 nm. So, we observe that a PL peak is blue-shifted from 510 nm to 465 nm in the NTRT-PL spectrum (Fig. 5(a) for the bared TNA film).

In the case of the Au NPs decorated TNA under no light irradiation, atmospheric molecular oxygen is adsorbed on the surface of the Au NPs. When metal NPs are deposited onto a semiconductor surface, a Schottky barrier is formed at the junction between the metal and the semiconductor due to the alignment of their different Fermi levels. Thus, it is reasonable to believe that the electron transfer from TiO_2 to Au NPs is facilitated. The surface energy band of the decorated TNA is bent resulting from the existence of the Schottky junction, just as presented in Fig. 7(b).

In the case of the Au NPs decorated TNA under UVC light irradiation, plenty of electrons are excited from the valence band to the conduction band, in consideration of the fact that the energy of the incident photons (4.7 eV) is much higher than the energy gap of TiO_2 (3.2 eV). Due to the difference in the work function between Au (5.3 eV) and TiO_2 (4.7 eV), it is reasonable that the electrons transfer from the conduction band of TiO_2 to the Au NPs with a large driving force until an equilibrium is reached.[33] This results in the suppression of the electron–hole recombination. The photo-excited holes diffuse to the semiconductor surface to combine with the water adsorbed onto the TiO_2 surface, leading to the formation of hydroxyl radicals (·OH); while the electrons can react with O^2 to generate superoxide anions ($\cdot O^{2-}$).[19,34,35] The photo-induced electron transfer and photocatalytic processes are shown in Fig. 7(c).

Transiently after the UVC light irradiation, the TNA–Au NPs system no longer generates photo-induced electron–hole

pairs. On the one hand, a large amount of photo-generated electrons are consumed in the surface photocatalytic process, which relies on the driving force of the built-in electric field at the interface of Au NPs and TNA. The concentration of electrons in the conduction band of TiO_2 is therefore much decreased in comparison with the case of the pristine TiO_2. The metal NPs therefore, are able to play a key role in the combined processes of photocatalytic charge transfer and efficient charge separation, and so suppressing the recombination of the photo-generated electron–hole pairs can be achieved. On the other hand, the electron in the conduction band of TiO_2, which is excited by the UVC light irradiation, can recombine with the holes. Obviously, there is a competitive relationship between the photocatalytic process and the photo-generated charge recombination process, which both contribute to the electron dissipation in TiO_2.

Figure 8 shows the amounts of peak blue shift in the NTRT-PL spectra with different Au NPs sputtering times of 0 s, 10 s, 20 s, 40 s, and 60 s. At the sputtering time of 0 s, i.e., the TNA without Au NPs, there is only the recombination process of the photo-generated electron–hole pairs. For this case, the concentration of electrons in the conduction band of TiO_2 is maximum, apparently causing the reaction $F^+ + e^- \rightarrow F$, and the PL peak shifts from 510 nm to 465 nm with the evolution of time, the amount of peak blue shift is 45 nm. When the Au sputtering time is 10 s, the concentration of adsorbed oxygen molecules is more than that in the pristine TiO_2. Because of the co-existence of recombination process and photocatalytic process, the concentration of electrons in the conduction band of TiO_2 is consequently lower than that in the former case. The reaction $F^+ + e^- \rightarrow F$ can still occur, yet the peak shifts from 498 nm to 465 nm, and the amount of peak blue shift is lowered to about 33 nm. When the Au sputtering time is 20 s, the concentration of adsorbed oxygen molecules is increased due to the increased amount of Au NPs, and the photocatalytic process consumes an increased number of electrons in the conduction band. Therefore, the concentration of electrons in the conduction band of TiO_2 is lower than that for the sputtering time of 10 s. The PL peak shifts from 486 nm to 465 nm, and the amount of peak blue shift is lowered to about 21 nm. When the Au sputtering time is 40 s, most electrons in the conduction band are consumed in the photocatalytic process, and the reaction $F^+ + e^- \rightarrow F$ does not occur, thus almost no peak shift is experimentally detectable. At last, for the Au sputtering time of 60 s, the size of the Au NPs is the largest among all the studied cases; however, the coverage of Au NPs becomes quasi-continuous, which introduces an extrinsically lowered surface area for oxygen adsorption. It therefore leads to the abnormal increase of OV defect sites at a rather large Au coverage (60 s). So, the consumption capacity of electrons in the conduction band recombination process again is comparable with that in the photocatalytic process; the reaction $F^+ + e^- \rightarrow F$ occurs again, the peak shifts from 494 nm to 465 nm, and the amount of peak blue shift is 29 nm.

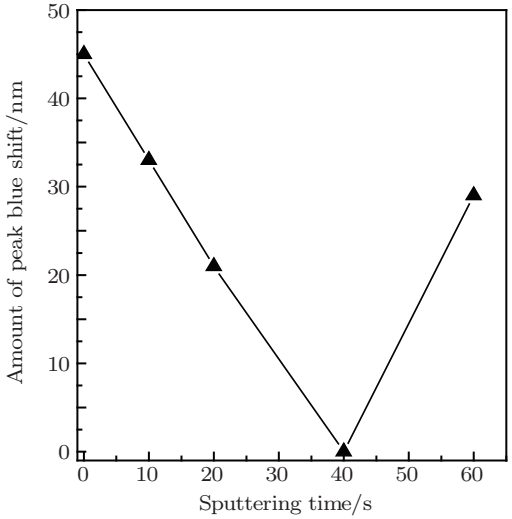


Fig. 8. Peak blue shift versus the Au NPs sputtering time.

In order to check the proposed mechanism, the photocatalytic performances of the pristine TNA and the Au NPs decorated TNA films are investigated. UV irradiation at 254 nm is used, which is close to the wavelength of 266 nm for the transient PL study. Figure 9 shows the intrinsic photo-degradation efficiency of MO under UV lamp irradiation, comparing the photocatalytic performances of the pristine TNA and the Au NPs decorated TNA films with different sputtering times.

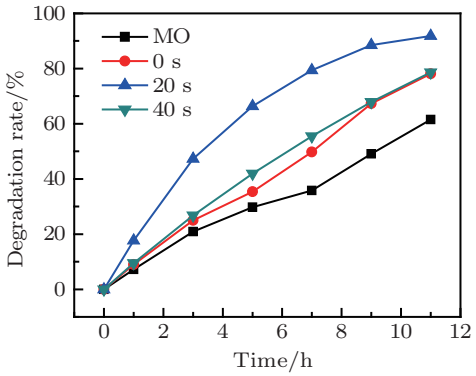


Fig. 9. (color online) Photo-degradation efficiency of MO, pristine TNA, and Au NPs decorated TNA films with different sputtering times of 20 s and 40 s.

Under the UV irradiation for 11 h, the photo-degradation ratio for the intrinsic MO aqueous solution is about 50%, and the MO photo-degradation ratio for the Au NPs decorated TNA films (0 s and 40 s) is about 75%, while that for the other Au NPs decorated TNA film (20 s) is about 90%. It clearly shows the enhanced photocatalytic ability of the Au NPs decorated TNA films, and this experimental result well supports the above-suggested ultrafast charge transfer dynamics between Au NPs and TNA under UV excitation.

4. Conclusion

In summary, highly ordered anodic oxidation anatase-dominated phase TNA films decorated with Au nanoparticles exhibit a strongly enhanced photocatalytic activity under the illumination of UVC light. The electric field in the Schottky nano junctions between the metal NPs and the semiconductor drives electrons to transfer from the conduction band of TiO_2 to the Au NPs until an equilibrium is reached, which results in a significant improvement in the photocatalytic performance. This proposal is supported by the characterizations of NTRT-PL spectra and steady-state PL spectra, which distinctly reveal the competitive relationship between the recombination process of the photo-generated charge carriers and the surface photocatalytic process. Well designed experiments show an enhanced UV photocatalysis ability of the Au NPs decorated TNA film. We believe that the configuration and fabrication method used for the photocatalyst preparation in this work not only provides new insights into the fabrication of a high performance photocatalyst to meet the requirements of future green environmental and energy technologies, but also opens up new prospects for the development of metal NPs-enhanced photoelectric devices.

References

[1] Paramasivam I, Macak J M and Schmuki P 2008 *Electrochemistry Communications* **10** 71
[2] Park J H, Lee T W and Kang M G 2008 *Chemical Communications* **25** 2867
[3] Yao D D, Field M R, O'Mullane A P, Kalantar-zadeh K and Ou J Z 2013 *Nanoscale* **5** 10353
[4] Wang X, Zhang Y, Deng H H, Shen Y C, Lu Z H and Cui Y P 2001 *Chin. Phys.* **10** 54
[5] Liu M, Zhao G H, Tang Y T, Shi H J and Yang N J 2013 *Chinese Journal of Chemistry* **31** 215
[6] Fujishima A and Honda K 1972 *Nature* **238** 37
[7] Anpo M, Dohshi S, kitano M, Hu Y, Takeuchi M and Matsuoka M 2005 *Annu. Rev. Mater. Res.* **35** 1
[8] Shi J Y, Chen J, Feng Z C, Chen T, Lian Y X, Wang X L and Li C 2007 *J. Phys. Chem. C* **111** 693
[9] Choudhury B and Choudhury A 2013 *Current Applied Physics* **13** 1025
[10] Gordon T R, Cargnello M, Paik T, Mangolini F, Weber R T, Fornasiero P and Murray C B 2012 *J. Am. Chem. Soc.* **134** 6751
[11] Pan X, Zhang N, Fu X and Xu Y 2013 *J. Appl. Catal. A* **453** 181
[12] Chen P and Zhang X 2008 *Clean: Soil, Air, Water* **36** 507
[13] Li Q Y, Wang K, Zhang S L, Zhang M, Yang J J and Jin Z S 2006 *J. Mol. Catal. A* **258** 83
[14] Du Z, Feng C, Li Q, Zhao Y and Tai X 2008 *Colloids Surf. A* **315** 254
[15] Cao Y, Tan H, Shi T, Tang T and Li J 2008 *J. Chem. Technol. Biotechnol.* **83** 546
[16] Wang Q, Pan Y Z, Huang S S, Ren S T, Li P and Li J J 2011 *Nanotechnology* **22** 025501
[17] Zou Z Y, Wang Q, Chen X J and Qu S L 2009 *J. Appl. Phys.* **105** 103114
[18] Nagaveni K, Hegde M S and Madras G 2004 *J. Phys. Chem. B* **108** 20204
[19] Lu Y, Yu H T, Quan X and Zhao H M 2012 *Environmental Science & Technology* **46** 1724
[20] Radecka M, Zakrzewska K, Czternastek H, Stapinski T and Debrus S 1993 *Appl. Surf. Sci.* **65** 227
[21] Kollbek K, Sikora M, Kapusta C, Szlachetko J, Zakrzewska K, Kowalski K and Radecka M 2013 *Appl. Surf. Sci.* **281** 100
[22] Subramanian V, Wolf E E and Kamat P V 2004 *J. Am. Chem. Soc.* **126** 4943
[23] Pearson A, Zheng H D, Kalantar-zadeh K, Bhargava S K and Bansal V 2012 *Langmuir* **28** 14470
[24] Feil A F, Migowski P, Scheffer F R, Pierozan M D, Corsetti R R, Rodrigues M, Pezzi R P, Machado G, Amaral L, Teixeira S R, Weibel D E and Dupont J 2010 *Journal of the Brazilian Chemical Society* **21** 1359
[25] Chen C C, Ma W H and Zhao J C 2010 *Chemical Society Reviews* **39** 4206
[26] Liu L Z, Xu W, Wu X L, Zhang Y Y, Chen T H and Chu P K 2012 *Appl. Phys. Lett.* **100** 121904
[27] Zeng H B, Duan G T, Li Y, Yang S K, Xu X X and Cai W P 2010 *Advanced Functional Materials* **20** 561
[28] Chang Y H, Liu C M, Chen C and Cheng H 2012 *Journal of the Electrochemical Society* **159** 401
[29] Pan X Y and Xu Y J 2013 *Applied Catalysis A: General* **459** 34
[30] Devi L G and Kavitha R 2013 *Applied Catalysis B: Environmental* **140** 559
[31] Das K, Sharma S N, Kumar M and De S K 2009 *J. Phys. Chem. C* **113** 14783
[32] Serpone N, Lawless D and Khairutdinov R 1995 *J. Phys. Chem.* **99** 16646
[33] Yu H B, Wang X H, Sun H W and Huo M X 2010 *Journal of Hazardous Materials* **184** 753
[34] Lu Y, Chen S, Quan X and Yu H T 2011 *Chinese Journal of Catalysis* **32** 1838
[35] Li C Y, Wang J B and Wang Y Q 2012 *Chin. Phys. B* **21** 098102